Enzyme Deactivation Due to Metal-Ion Dissociation during Turnover of the Cobalt-β-Lactamase Catalyzed Hydrolysis of β-Lactams†

Adriana Badarau and Michael I. Page*

Department of Chemical and Biological Sciences, University of Huddersfield, Queensgate, Huddersfield HD1 3DH, U.K.

Received May 22, 2006; Revised Manuscript Received July 11, 2006

ABSTRACT: Metallo-β-lactamases are native zinc enzymes that catalyze the hydrolysis of β-lactam antibiotics but are also able to function with cobalt (II) and require one or two metal ions for catalytic activity. The kinetics of the hydrolysis of benzylpenicillin catalyzed by cobalt substituted β-lactamase from *Bacillus cereus* (BcII) are biphasic. The dependence of enzyme activity on pH and metal-ion concentration indicates that only the di-cobalt enzyme is catalytically active. A mono-cobalt enzyme species is formed during the catalytic cycle, which is virtually inactive and requires the association of another cobalt ion for turnover. Two intermediates with different metal to enzyme stoichiometries are formed on a branched reaction pathway. The di-cobalt enzyme intermediate is responsible for the direct catalytic route, which is pH-independent between 5.5 and 9.5 but is also able to slowly lose one bound cobalt ion via the branching route to give the mono-cobalt inactive enzyme intermediate. This inactivation pathway of metal-ion dissociation occurs by both an acid catalyzed and a pH-independent reaction, which is dependent on the presence of an enzyme residue of pK_a = 8.9 ± 0.1 in its protonated form and shows a large kinetic solvent isotope effect (H_2O/D_2O) of 5.2 ± 0.5, indicative of a rate-limiting proton transfer. The pseudo first-order rate constant to regenerate the di-cobalt β-lactamase from the mono-cobalt enzyme intermediate has a first-order dependence on cobalt-ion concentration in the pH range 5.5−9.5. The second-order rate constant for metal-ion association is dependent on two groups of pK_a 6.32 ± 0.1 and 7.47 ± 0.1 being in their deprotonated basic forms and one group of pK_a 9.48 ± 0.1 being in its protonated form.

The major bacterial defense mechanism against β-lactam antibiotics consists of producing a class of enzymes, the β-lactamases, which catalyze the hydrolysis of the β-lactam ring, rendering the drugs inactive (Scheme 1). From a mechanistic point of view, β-lactamases are divided into two classes: serine β-lactamases, (classes A, C, and D β-lactamases), which use an active site serine residue for hydrolysis, and metallo-β-lactamases, (MBLs[1]), (class B β-lactamases), which require one or two zinc ions for catalytic activity. MBLs have no sequence or structural homology with serine β-lactamases and exhibit a broad spectrum substrate profile, including some mechanism based inhibitors of class A β-lactamases (*1*). MBLs have been further divided into three subclasses, B1, B2, and B3 (*2*), on the basis of their amino acid sequences, substrate profile, and metal-ion requirement. The largest group is B1 and contains four well-studied β-lactamases: BcII from *Bacillus cereus* (*3*−*5*), CcrA from *Bacteroides fragilis* (*6*−*9*), IMP-1 from *Pseudomonas aeruginosa* (*10*−*12*), and BlaB from *Cryseobacterium meningosepticum* (*13*). These enzymes efficiently hydrolyze a wide range of substrates, including penicillins, cephalosporins, and carbapenems (*14*).

Scheme 1

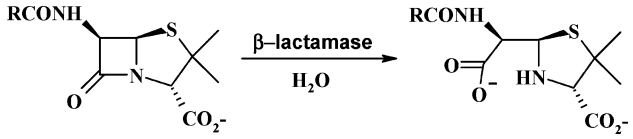

The evidence for two zinc binding sites on the enzymes is well established (*2*−*4*, *6*, *12*, *13*), but the zinc ligands in the two sites are not the same and are not fully conserved between the different MBLs. In subclass B1 enzymes such as the *Bacillus cereus* enzyme, BcII, the zinc in site 1 (the histidine site or His_3 site) is tetracoordinated by the imidazoles of three histidine residues (116, 118, and 196) and a water molecule, Wat_1. Zinc is pentacoordinated in site 2 by His263, Asp120, Cys221, and one water molecule; the fifth ligand at site 2 is carbonate (*15*) or water, Wat_2 (*3*, *6*, *16*, *17*). In one crystal structure (*15*), Wat_2 is missing and also in structures with inhibitors bound (*12*). The distance between two metal ions varies from 3.4 to 4.4 Å in different structures of the BcII and CcrA enzymes (*3*, *6*, *15*−*17*). Several structures of the CcrA enzyme show a bridging water ligand between the two metals, which is thought to exist as a hydroxide ion (*6*, *17*). Also, in a structure of BcII containing two zinc ions determined at pH 7.5, there is a similar bridging

† This research was supported by the European Union research network on metallo-β-lactamases within the Training and Mobility of Researchers (TMR) Program, contract number HPRN-CT-2002-00264 and the University of Huddersfield.

* To whom correspondence should be addressed. Phone: +1484 472169. Fax: +1484 472182. E-mail: m.i.page@hud.ac.uk.

[1] Abbreviations: MBL, metallo-β-lactamases; BcII, *Bacillus cereus*-β-lactamase; CcrA, *Bacteroides fragilis*-β-lactamase; NMR, nuclear magnetic resonance; EPR, electron paramagnetic resonance; PAC, perturbed angular correlation; LMCT, ligand to metal charge transfer; MCD, magnetic circular dichroism; MES, 2-[*N*-morpholino]ethanesulfonic acid; MOPS, 3- [*N*-morpholino]propanesulfonic acid; TAPS, *N*-tris[hydroxymethyl]methyl-3-aminopropanesulfonic acid; CHES, 2-[*N*-cyclohexylamino]ethanesulfonic acid; EDTA, ethylenediaminetetraacetic acid.

10.1021/bi0610146 CCC: $33.50
Published on Web 08/18/2006

water molecule (*18*), but in structures of this enzyme at lower pH, this solvent molecule is strongly associated with the zinc in site 1 (*3*).

The binding affinities and the dependence of the catalytic activity of MBLs on the two zinc ions are different. BcII has very different dissociation constants for the two metal binding sites, which for the loss of the metal ion from the mono-zinc enzyme, K_{mono}, is 6.2×10^{-10} M, whereas that from di-zinc MBL, K_{di}, is 1.5×10^{-6} M (*19*). In the presence of imipenem as substrate, K_{mono} decreases significantly, from nM to pM, whereas K_{di} decreased only 2-fold (*20*). This suggests that the mono-zinc enzyme is responsible for the catalytic activity under physiological conditions, where the concentration of free Zn^{2+} is in the pM region. In contrast, class B1 CcrA from *Bacteroides fragilis* binds both zinc ions very tightly (*21*), and in early kinetic studies of CcrA, it was proposed that both the mono- and the di-zinc forms of the enzyme were catalytically active, with slightly different activities (*7*). However, later studies have shown that only the di-zinc species is active and that the previously observed mono-zinc CcrA was a mixture of the di-zinc and the apo (metal free) enzyme (*22*). The mechanisms of action of metallohydrolases that require two metal ions to catalyze the hydrolysis of amides and esters of carboxylic and phosphoric acids have been recently reviewed (*23*). The main function of the metal ions are to activate aqua/hydroxo bridging or terminal ligands for nucleophilic attack and to act as Lewis acids to stabilize the negative charge developed on the substrate in the transition state.

The exchange of the spectroscopically silent zinc with probes, such as cobalt, copper, and cadmium, enables the study of the interactions of the metal ion in the enzyme active site with ligands, substrates, and inhibitors, using techniques such as UV−Vis, NMR, EPR, and PAC spectroscopy (*24*−*26*). The zinc of metallo β-lactamases can be exchanged with cadmium, cobalt, and manganese to give catalytically active enzymes (*27*−*29*). The use of a combination of NMR and PAC spectroscopy to study cadmium binding to *Bacillus cereus* MBL has revealed a rapid intramolecular exchange of the metal between the two sites in the mono-cadmium enzyme and negative cooperativity in metal binding (*29*). The enzyme inhibitor (*R*)-thiomandelate induces a very strong positive cooperativity for binding the second cadmium cation (*30*). The UV−Vis spectra of the di-cobalt substituted class B1 metallo-β-lactamases CcrA from *Bacteroidis fragilis* (*21*, *31*) and BcII from *Bacillus cereus* (*4*, *32*) show an intense sulfur to Co(II), ligand to metal, charge transfer (LMCT) band.

Bicknell and Waley (*33*) observed that the progress curves for the cobalt substituted BcII catalyzed hydrolysis of benzylpenicillin are biphasic, with an initial burst followed by a steady-state rate. The size of the burst was greater than the concentration of enzyme, which led the authors to propose a branched kinetic hydrolysis scheme with two kinetically indistinguishable pathways (Scheme 2). Two enzyme−substrate intermediates, ES^1 and ES^2, were characterized on the basis of their UV−Vis (*33*) and MCD (*34*) spectra. ES^1 showed a large increase in the Cys-Co LMCT compared with that of both the free enzyme and ES^2. The MCD spectra suggested a change in the coordination number of the active site metal during the reaction, that is, from five-coordinated in the free enzyme to four-coordinated in ES^1 and subsequently five-coordinated in ES^2. The authors concluded that ES^1 and ES^2 are noncovalent enzyme−substrate complexes, interconvertible by a reversible conformational change. These studies were performed at saturating concentrations of cobalt ion. However, more recent studies (*35*) have shown that the activity of ZnBcII is metal-ion concentration dependent at low pH, and we suspected that the biphasic kinetics may be due to the relationship between the enzyme and the metal ion, rather than due to a conformational change. We therefore studied the pH rate profiles for CoBcII at different cobalt-ion concentrations in order to elucidate the nature of the intermediates. Cobalt has about 100 fold less affinity than zinc for the two binding sites of BcII, which makes it more convenient from an experimental point of view for studying the differences between the catalytic properties of the enzyme with one and two metal ions. Furthermore, the microscopic rate constants for the association of the first and the second cobalt ions to BcII are 50- and 20-fold, respectively, less than those for zinc binding (*19*). Herein, we report some unusual kinetic properties of CoBcII as a result of a complex catalytic pathway that results in the loss of a metal ion during catalytic turnover, leading to the formation of an inactive enzyme species.

Scheme 2

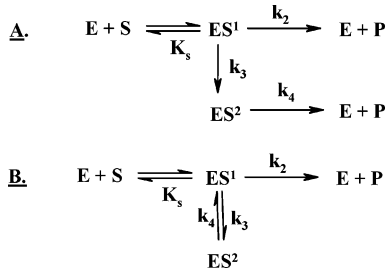

EXPERIMENTAL PROCEDURES

Materials. The reagents used in all kinetic experiments were analytical or of an equivalent grade. Buffers, benzylpenicillin, Chelex 100, and $CoCl_2$ (99.9999%) were purchased from Sigma. D_2O, NaOD, and DCl were obtained from Goss Scientific, Ltd. Deionized ultrapure water (18 M Ω cm) was used for the preparation of buffers and other aqueous solutions. The buffers used were acetate (pK_a 4.75), MES (pK_a 6.15), MOPS (pK_a 7.20), TAPS (pK_a 8.40), and CHES (pK_a 9.2). Buffer solutions were prepared just prior to the experiment, and their ionic strength was kept constant by means of potassium chloride. Special care was taken to ensure metal-free conditions (*5*); buffers were stirred overnight with 2 g of Chelex 100 per 100 mL buffer solution.

The metallo-β-lactamase (BcII from *Bacillus cereus* 569/H/9) was supplied as an aqueous suspension in a 10 mM MES buffer by Dr. Christian Damblon (University of Leicester, U.K.). The apo *Bacillus cereus* 569/H/9 enzyme (metal-free BcII) was prepared by the following procedure: ZnBcII was dialyzed, while stirring, against two changes of 0.015 M MES at pH 6.5, containing 0.1 M NaCl and 0.02M EDTA over a 12 h period; EDTA was removed from the resulting apoenzyme solution by four dialysis steps against the same buffer containing 1 M NaCl and Chelex 100 and finally two dialysis steps against 0.015 M MES at pH 6.5

containing 0.1 M NaCl and Chelex 100. The resulting apoenzyme contained less than 3% Zn^{2+}, as determined by atomic absorption spectroscopy, and less than 10% free EDTA, as shown by ^{1}H NMR. The apoenzyme concentration was determined using the reported extinction coefficient, ϵ_{280} = 30 500 M^{-1} s^{-1} (*19*). Addition of zinc to the apoenzyme restored 90% of the initial enzymatic activity.

Equipment. pH Measurements were made using a ϕ40 pH meter (Beckman, Fullerton, U.S.A.) with a calomel glass electrode (Beckman). A two point calibration of the pH meter was taken at 30 °C prior to use, with a pH 7 phosphate green buffer (Beckman) and a pH 4 or pH 10 calibration buffer (BDH, Poole, U.K.). The pD values were taken as pH meter readings of +0.40.

UV spectrometry was carried out on a Cary 1E UV−visible spectrometer equipped with a twelve compartment cell block thermostated by using a peltier system (Varian, Australia). Rate constants were estimated using the Cary Win UV kinetics application, version 02.00 (*26*).

The residual zinc content of apoBcII was determined by atomic absorption spectroscopy on a Perkin-Elmer Analyst 100 Atomic absorption Spectrometer. The hollow cathode lamp wavelength was set at 213.9 nm, with a current of 7 mA, and a slit wave of 0.7 nm. Zinc sulfate solutions of different concentrations were used as standards.

Pre-Steady-State Kinetics. The pre-steady-state kinetic studies were performed at 5 °C. Unless otherwise specified, the reaction was started by adding a solution (10−20 μL) containing CoBcII and excess $CoCl_2$ (final concentrations in the assay cell $[Co^{2+}] = 7.5 \times 10^{-6}-5 \times 10^{-3}$ M and [apoBcII] = $1.25 \times 10^{-7}-6 \times 10^{-6}$ M) to a buffer solution (2 mL) containing benzylpenicillin ($2.5 \times 10^{-4}-1 \times 10^{-3}$ M). Cobalt substituted BcII containing excess $CoCl_2$ was prepared by incubating apo-BcII ($2.5 \times 10^{-6}-6 \times 10^{-4}$ M) and $CoCl_2$ ($10^{-5}-10^{-1}$ M) in 10 mM MES at pH 6.5 for 5 min at room temperature, prior to each experiment. The rate of hydrolysis was followed by monitoring the decrease in absorbance at 235 nm ($\Delta\epsilon$ = 820 cm^{-1}) and was recorded approximately 3 s after the injection of metalloenzyme and excess metal-ion salt. The resulting biphasic progress curves were fitted to eq 1, using SCIENTIST software, where p is the concentration of product at time t, R is the observed first-order rate constant characterizing the transient, B is the burst, V is the final steady-state rate (*33*), and t_0 is the time elapsed from the beginning of the reaction to the moment it is recorded.

The microscopic rate constants k_2, k_3, and k_4 of Scheme 2 were calculated from the R, B, and V parameters for both potential pathways of Scheme 2, A and B, as described previously (*33*).

$$p = V(t + t_0) + B(1 - e^{-R(t+t_0)}) \quad (1)$$

It can be shown that under the assumption that $k_1[S] \gg$ (k_2 and k_3), (where $K_s = k_{-1}/k_1$), for both pathways $k_2 = (V + RB)/e_0$ and $k_3 + k_4 = R$, and for mechanism A, k_4 is calculated from the equation $k_4^2 - (k_2 + R)k_4 + RV/e_0 = 0$, whereas for mechanism B, $k_4 = RV/(k_2e_0)$, where e_0 is the total metalloenzyme concentration used.

The derived values of k_2 and k_3 for each pH/pD are the average of at least six experiments performed at different metal-ion and different apoenzyme concentrations. The measured values for k_4 were found to vary with cobalt-ion concentration: $k_4 = k'_4[Co^{2+}]$; the second-order rate constant, k'_4, was determined from the plot of the first-order rate constant, k_4, against cobalt-ion concentration (3−5 different cobalt-ion concentrations were used for each pH/pD).

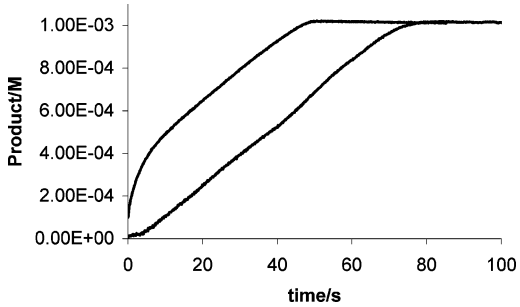

FIGURE 1: Progress curve of CoBcII catalyzed hydrolysis of benzylpenicillin (1×10^{-3} M) in 0.025 M MES (I = 0.25 M at pH 6.7, at 5 °C) (in the assay cell, $[Co^{2+}] = 2 \times 10^{-4}$ M, [apoBcII] = 3×10^{-6} M). Upper line: reaction started by adding a solution of CoBcII and excess $CoCl_2$ (20 μL) to a solution of benzylpenicillin in buffer (2 mL); lower line: reaction started by adding apoBcII (20 μL) to a solution of benzylpenicillin and $CoCl_2$ in buffer (2 mL).

RESULTS AND DISSCUSION

The hydrolysis of benzylpenicillin (1) by cobalt substituted BcII was followed at 5 °C, by monitoring the decrease in UV absorbance at 235 nm corresponding to the depletion of substrate. When the reaction is started by adding a mixture of CoBcII and excess Co^{2+} ([apoBcII] = 3×10^{-6} M, $CoCl_2$ = 2×10^{-4} M) to a solution of benzylpenicillin (1×10^{-3} M) in buffer at pH = 6.7, there is an initial burst (5−10 s), followed by a transition to a steady-state rate (Figure 1, upper line), in agreement with the previous observations of Bicknell and Waley (*33*). A similar hydrolysis profile is obtained when the reaction is started by adding benzylpenicillin (1×10^{-3} M) to a solution of apoBcII (3×10^{-6} M) and $CoCl_2$ (2×10^{-4} M), previously incubated for 1 min in buffer. However, if the reaction is started by adding apoBcII (3×10^{-6} M) to a solution of $CoCl_2$ (2×10^{-4} M) and benzylpenicillin (1×10^{-3} M) in buffer or by adding $CoCl_2$ (2×10^{-4} M) to a solution of apoBcII (3×10^{-6} M) and benzylpenicillin (1×10^{-3} M) in buffer, there is no apparent burst but a short lag in the first few seconds of the reaction, followed by a steady-state rate, which is equal to the steady-state rate following the burst in the previous cases (Figure 1, lower line). This appears to suggest that metal-ion binding to the enzyme limits the rate in some way and is indicative of a kinetically and thermodynamically controlled partitioning between the apo, mono- and di-cobalt forms of the enzyme.

Because there was no observable change in absorbance at 235 nm on mixing the apoenzyme with cobalt chloride and the size of the burst was about 100 fold larger than the enzyme concentration, it follows then that the absorbance change is due to product formation and not the accumulation of an enzyme−substrate intermediate. The initial faster rate followed by a slower one after about 25% conversion of the substrate indicates the generation of a less active but more stable catalyst.

The burst is only apparent when the reaction is started with cobalt enzyme (apoenzyme previously incubated with

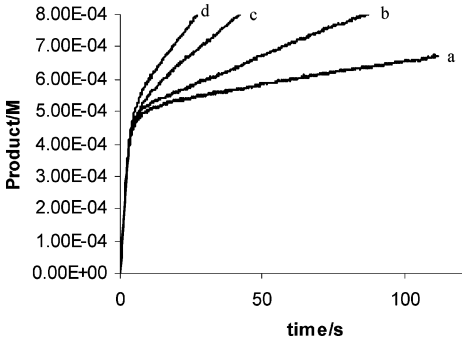

FIGURE 2: Progress curves of CoBcII catalyzed hydrolysis of benzylpenicillin (10^{-3} M) in 0.025 M MES (I = 0.25 M at pH 5.92, at 5 °C) (in the assay cell, [apoBcII] = 6×10^{-6} M and various Co^{2+} concentrations (a) = 2.5×10^{-4} M, (b) = 5×10^{-4} M, (c) = 1×10^{-3} M, (d) = 2×10^{-3} M).

$CoCl_2$), suggesting that the cobalt enzyme species responsible for the initial fast rate is not formed, or is forming slowly, under the conditions of the experiment initiated by adding apoenzyme to a solution of cobalt chloride and substrate. Benzylpenicillin does not measurably bind to the apoenzyme (*36*), and thus, it is unlikely to hinder cobalt association. The binding of the first cobalt ion to the apoenzyme is expected to be completed in the dead time of the experiment, approximately 3 s, because the calculated half-life is 0.013 s (the estimated pseudo first-order rate constant for the binding of the first cobalt ion, k_{obs}, is 56 s^{-1}, for 2×10^{-4} M [Co^{2+}] at pH 7.0 at 25 °C, using the reported second-order rate constant (*19*)). Because the association of the second cobalt ion is at least 10-fold slower than that of the first cobalt ion (*19*), it is likely that the relatively slow formation of the di-cobalt enzyme is causing the absence of the burst in the experiment started with apoenzyme, implying that the di-cobalt BcII species is responsible for the initial fast rate observed when the reaction was initiated with the cobalt enzyme and excess cobalt ion.

The fact that adding benzylpenicillin to a solution of CoBcII and excess Co^{2+} in buffer gives the same initial burst of hydrolysis as that seen when the reaction is initiated by adding a mixture of CoBcII and excess Co^{2+} to a solution of benzylpenicillin in buffer suggests that at equilibrium (at pH 6.7 and 5 °C) and for the metal and apoenzyme concentrations used, most of the enzyme is present in its most active form, that is, the di-cobalt form. The previous study of CoBcII catalyzed hydrolysis of benzylpenicillin at low temperatures used a single concentration of $CoCl_2$ (10^{-3} M), for which maximum catalytic activity is achieved (*33*).

To see if the interconversion of mono-cobalt and di-cobalt enzyme species was responsible for the unusual kinetic behavior, we compared the biphasic progress curves of CoBcII catalyzed hydrolysis of benzylpenicillin at different metal-ion concentrations. At pH 5.9, it is clear that both the magnitude and the rate of the initial burst are independent of the external cobalt-ion concentration, whereas the steady-state rate varies proportionally to the metal-ion concentration (Figure 2).

Bicknell and Waley accounted for the branched kinetics by the kinetically undistinguishable pathways A and B (Scheme 2), which differ by the fact that in A, both ES^1 and ES^2 species yield product, whereas in B, only ES^1 yields product, and the presumed conformational change is reversible (*33*, *34*). ES^1 was considered to be the most reactive form of the enzyme and ES^2 to be less reactive. The direct route via ES^1, with rate constant k_2, corresponds to the burst, and subsequently, the rate decreases as a result of the formation of ES^2 via the branching pathway, with rate constant k_3.

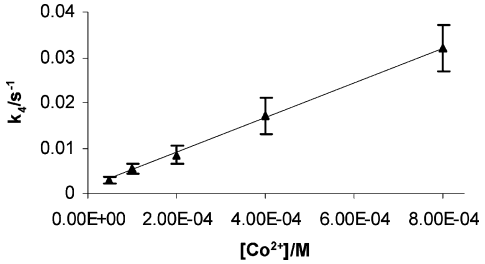

FIGURE 3: Plot of the calculated first-order rate constant k_4 against cobalt-ion concentration for the CoBcII catalyzed hydrolysis of benzylpenicillin (10^{-3} M) in 0.025 M MES (I = 0.25 M at pH 6.30, at 5 °C) (in the assay cell, [apoBcII] = 6×10^{-6} M).

The biphasic progress curve for the CoBcII catalyzed hydrolysis of benzylpenicillin at 5 °C was studied at different metal-ion, apoenzyme, and substrate concentrations, over the pH range 5.4−9.8, in H_2O and D_2O. In all cases, the reaction was initiated by adding CoBcII and excess $CoCl_2$ to a solution of benzylpenicillin in buffer. The microscopic rate constants k_2, k_3, and k_4 (Scheme 2) were calculated as described in the Experimental Procedures section, and the values found were similar for the two mechanisms considered. Also, they were found to be independent of apoenzyme and substrate concentrations and, except for k_4, of external cobalt-ion concentration for a given pH (pD). Varying the buffer concentration from 0.025 to 0.1 M while keeping the pH and the ionic strength (0.25 M) constant had no effect on the magnitude of k_2, k_3, and k_4. The first-order rate constant k_4 was found to be proportional to the cobalt-ion concentration (Figure 3) for all pH (pD) values studied. The slope of this plot gives the apparent second-order rate constant k'_4, which is 37.7 M^{-1} s^{-1} at pH 6.3.

A background hydrolysis rate of benzylpenicillin in the presence of apoenzyme was determined for every pH and was insignificant. Also, both the burst and the steady-state rates (B and V) were directly proportional to the enzyme concentration used, indicating that the contribution of any cobalt−zinc heteroenzyme species (whose concentration would be limited by the concentration of residual zinc) to the observed rate of hydrolysis is negligible, and therefore, the measured catalytic activity corresponds to that of the holo-cobalt BcII enzyme.

(i) Rate Constant k_2. The microscopic first-order rate constant k_2 is independent of metal-ion concentration even at the lowest pH studied and essentially pH-independent between pH 5.4 and 9.9, with a value of 45 s^{-1}, although there is an apparent increase of less than 2-fold at higher pH. Similar behavior is seen in D_2O, where k_2 is pD independent from pD 5.4 to 8.5 with an average value of 32 s^{-1}, but it increases slightly, again less than 2-fold, at more basic pH. The solvent kinetic isotope effect $k_2^{H_2O}/k_2^{D_2O}$ is 1.4 ± 0.1.

(ii) Rate Constant k_3. The pH-dependence of the branching first-order rate constant k_3, which gives the less reactive form of the enzyme, is more complex (Figure 4) and shows a sigmoidal dependence as well as an apparent acid catalyzed

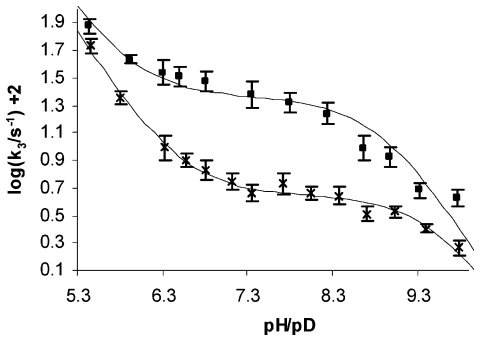

FIGURE 4: Plot of log k_3 against pH(■)/pD(x) for CoBcII catalyzed hydrolysis of benzylpenicillin (1×10^{-3} M) in 0.025 M buffer ($I = 0.25$ M, at 5 °C) (in the assay cell, [apoBcII] = 1.25×10^{-7}−1.2×10^{-5} M, [Co^{2+}] = 7.5×10^{-6}−1×10^{-2} M); the solid lines are the calculated values using eq 2 and the parameters shown in Table 1.

Scheme 3

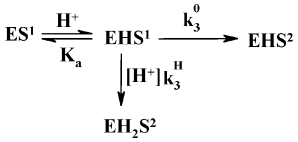

reaction. The former indicates the importance of an ionisable group of apparent pK_a 8.88, which is active in its acidic protonated form, EHS^1 (Scheme 3). It appears that the ionising group in EHS^1, responsible for the decrease in k_3 on the alkaline part of the pH-rate profile, may be also responsible for a slight increase in k_2 with increasing pH. The increase in k_3 below pH 7 (Figure 4) could be explained by an extension of mechanisms A or B (Scheme 2), with the inclusion of the EHS^1 species and a possible acid catalyzed conversion of the monoprotonated EHS^1 to the diprotonated EH_2S^2 species (Scheme 3).

The transformation of ES^1 to ES^2 occurs through the monoprotonated species EHS^1 via a pH independent and also an acid catalyzed degradation of EHS^1 with the corresponding first-order (k_3^0) and second-order (k_3^H) rate constants, respectively. The experimental data for both pH and pD k_3 profiles were fitted to eq 2, which quantifies the mechanism in Scheme 3, and the parameters obtained are shown in Table 1.

It makes chemical sense that if the reactive (ES^1) and less reactive (ES^2) forms of the enzyme correspond to the di- and mono-cobalt species, respectively, then the conversion of ES^1 to ES^2 occurs by a protonation step, presumably involving the protonation of a ligand required for the binding of the second cobalt ion.

$$k_3 = \frac{k_3^0 + k_3^H[H^+]}{1 + \frac{K_a}{[H^+]}} \qquad (2)$$

(iii) Rate Constant k_4. The first-order rate constant k_4 shows a first-order dependence on cobalt-ion concentration, which suggests that the second cobalt ion is required for turnover, probably by association to the mono-cobalt ES^2 enzyme species. The pH/pD dependence of the second-order rate constant, k'_4, measured as described in Experimental Procedures, is bell-shaped (Figure 5), with a maximum between pH/pD 8 and 9 of 1.22×10^3 M^{-1} s^{-1} in H_2O and 1.26×10^3 M^{-1} s^{-1} in D_2O (Table 1).

On the acidic limb, the rate decreases with a slope of 2, indicating that the deprotonation of two ionisable groups is required for maximum catalytic activity, as illustrated in Scheme 4. The experimental data were fitted to eq 3, where pK_{a2} and pK_{a1} correspond to the groups required in their deprotonated forms for activity, and pK_{a3} corresponds to the group required in its protonated form for activity, and the values found are shown in Table 1. Because the pseudo first-order rate constant k_4 shows a first-order dependence on cobalt-ion concentration, the corresponding second-order rate constant k'_{4max} (1.22×10^3 M^{-1} s^{-1} at the pH maximum, at 5 °C) could represent the rate of association of the metal ion to the ES^2 enzyme species. This is about 25-fold smaller than the reported rate of association of the second cobalt ion to the mono-cobalt enzyme, 3×10^4 M^{-1} s^{-1}, at 25 °C (*19*).

$$k_4 = \frac{k'_{4max}}{1 + \frac{[H^+]^2}{K_{a2}K_{a1}} + \frac{[H^+]}{K_{a1}} + \frac{K_{a3}}{[H^+]}} \qquad (3)$$

Proposed Mechanism

Considering the findings above, the original pathways proposed by Bicknell and Waley (*33*, *34*) (Scheme 2) can be reformulated as shown in Scheme 5, on the basis of the following.

(i) ES^1 Is a Di-Cobalt BcII−Substrate Complex (ECo_2S). ECo_2S gives a hydrolysis product with a catalytic rate constant k_2 that is pH-independent. ECo_2S can also lose one cobalt ion to give a catalytically unreactive mono-cobalt species, ECoS, with a branching rate constant k_3 that shows a dependence on both acid concentration and on an ionisable group in its acidic form (Scheme 6).

(ii) ES^2 Is a Mono-Cobalt Enzyme Species (ECoS or ECo). The fact that the rate constant k_4 shows a first-order dependence on metal-ion concentration over all of the pH range studied suggests that ES^2 is a mono-cobalt enzyme species.

ECoS is most likely formed by the slow release of one bound cobalt ion from the di-cobalt species ECo_2S. The very large solvent kinetic isotope effect of 5.2 of the pH-independent k_3^0 rate constant suggests that the loss of cobalt ion occurs through a rate-limiting step involving proton transfer and possibly more than one proton in-flight (*37*).

(iii) ES^2 Requires the Association of Another Cobalt Ion to Become Catalytically Active. ES^2 may be the mono-cobalt BcII−substrate complex ECoS, which is probably unable to turnover, but can accept a second cobalt ion either to yield back the ES^1 (ECo_2S) complex (Scheme 5, (B)), or to give a different di-cobalt BcII−substrate complex ES^3 (ECo_2S') (Scheme 5, (A)). There is no UV evidence for the formation of ES^3 (ECo_2S') (*33*, *34*), and if mechanism B occurs, ECo_2S' would, therefore, have to turnover very fast ($k_5 \gg$ (k_3 and k_4)). Another possibility is that ES^2 is the free mono-cobalt enzyme, ECo, generated from the fast turnover of ECoS. In this case, the metal dependent step k_4 corresponds to the association of the second metal ion to the free mono-cobalt

Table 1: Calculated Parameters of the Rate and Ionization Constants from Schemes 3 and 4

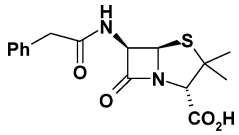

(1)

	k_3			k_4			
solvent	pK_a	k_3^0 (s^{-1})	k_3^H ($M^{-1}\,s^{-1}$)	pK_{a2}	pK_{a1}	pK_{a3}	k'_{4max} ($M^{-1}\,s^{-1}$)
H_2O	8.88 ± 0.12	0.23 ± 0.03	$(1.7 \pm 0.5) \times 10^5$	6.32 ± 0.13	7.47 ± 0.1	9.48 ± 0.1	$(1.22 \pm 0.11) \times 10^3$
D_2O	9.57 ± 0.07	$(4.4 \pm 0.2) \times 10^{-2}$	$(1.29 \pm 0.09) \times 10^5$	6.37 ± 0.14	8.07 ± 0.1	9.38 ± 0.2	$(1.26 \pm 0.24) \times 10^3$
H_2O/D_2O (Δ pK_a)	0.7 ± 0.2	5.2 ± 0.5	1.3 ± 0.2	-0.05 ± 0.27	0.6 ± 0.2	-0.1 ± 0.3	1.0 ± 0.2

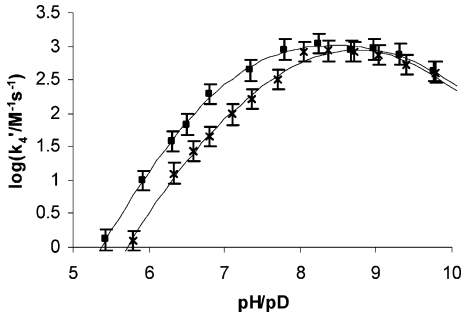

FIGURE 5: Plot of log k'_4 against pH(■)/pD(x) for CoBcII catalyzed hydrolysis of benzylpenicillin (1×10^{-3} M) in 0.025 M buffer ($I = 0.25$ M, at 5 °C) (in the assay cell [apoBcII] = 1.25×10^{-7}–6×10^{-6} M, [Co^{2+}] = 7.5×10^{-6}–4×10^{-3} M); the solid lines are the calculated values using eq 3 and the parameters shown in Table 1.

Scheme 4

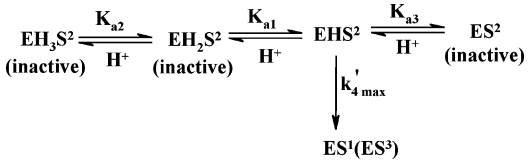

Scheme 5

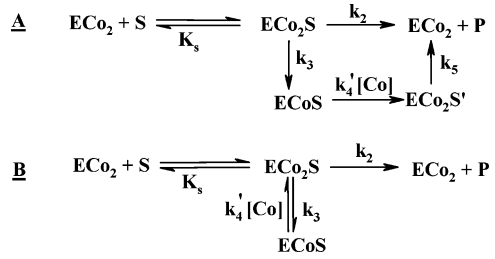

enzyme. This model implies that ECo is unable to bind the substrate and that the substrate only binds to the di-cobalt enzyme.

As k'_4 is pH-dependent, two groups on the mono-cobalt BcII species (ECoS) of pK_a 6.32 and 7.47 need to be deprotonated before the uptake of the second cobalt ion. The groups are, possibly, ligands for the incoming second cobalt ion. The existence of two protonation states of ES^2 (ECoS) species has been proposed before (*34*) on the basis of the observation that the UV spectrum of ES^2 at lower pH is different from that at high pH, where the charge-transfer absorption corresponding to the Cys−Co interaction is enhanced. Thus, it is possible that one of the two ionising groups is Cys221, the pK_a of which we have found

Scheme 6

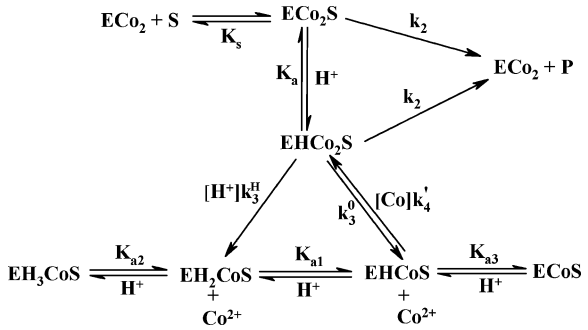

independently to be 7.85 (on basis of the measurement of the pH dependence of its alkylation rate with iodoacetamide) (*38*).

Arguments in favor of ES^1 being a di-cobalt enzyme species (ECo_2S) and ES^2 being a mono-cobalt enzyme species (ECoS) also come from previous spectroscopic studies (*34*). On the basis of the MCD spectra of ES^1 and ES^2 and the analogy with model compounds, it has been suggested that the cobalt ion coordination sphere is five-like in ES^2 and four-like in ES^1. Also, the Cys−Co charge-transfer band becomes 7-fold more intense in the ES^1 species compared with that of the ES^2 species (*34*), which may be explained by the fact that in ES^1, unlike in ES^2, the second cobalt ion is bound in the Cys site.

The proposed branched pathways involving the mono- and di-cobalt forms of the enzyme−substrate complex or intermediate ECoS and ECo_2S in their different protonation states are given in Scheme 6. Under the conditions of adding substrate to a solution of previously incubated enzyme and excess cobalt ion, the initial step involves the di-cobalt form of the enzyme binding the substrate to form the di-cobalt BcII−substrate complex (Scheme 6). The reaction is very fast, even at subzero temperatures (*33*), and under saturating conditions, it can be assumed that at time zero, all of the enzyme is present as ECo_2S. During turnover, ECo_2S reacts to give products via the fast route k_2 or can be converted to the mono-cobalt species, ECoS, with a rate constant k_3. When the regeneration of ECo_2S is much slower than branching ($k_4 \ll k_3$), at the steady-state, most of the enzyme will be in the ECoS form, and the rate-limiting step will be k_4. At higher metal-ion concentrations, when $k_4 \gg k_3$, most of the enzyme will be in the ECo_2S form, and the product will form via the rate-limiting step k_2. When k_3 and k_4 are of the same order of magnitude, the steady-state contains both ECo_2S

Scheme 7

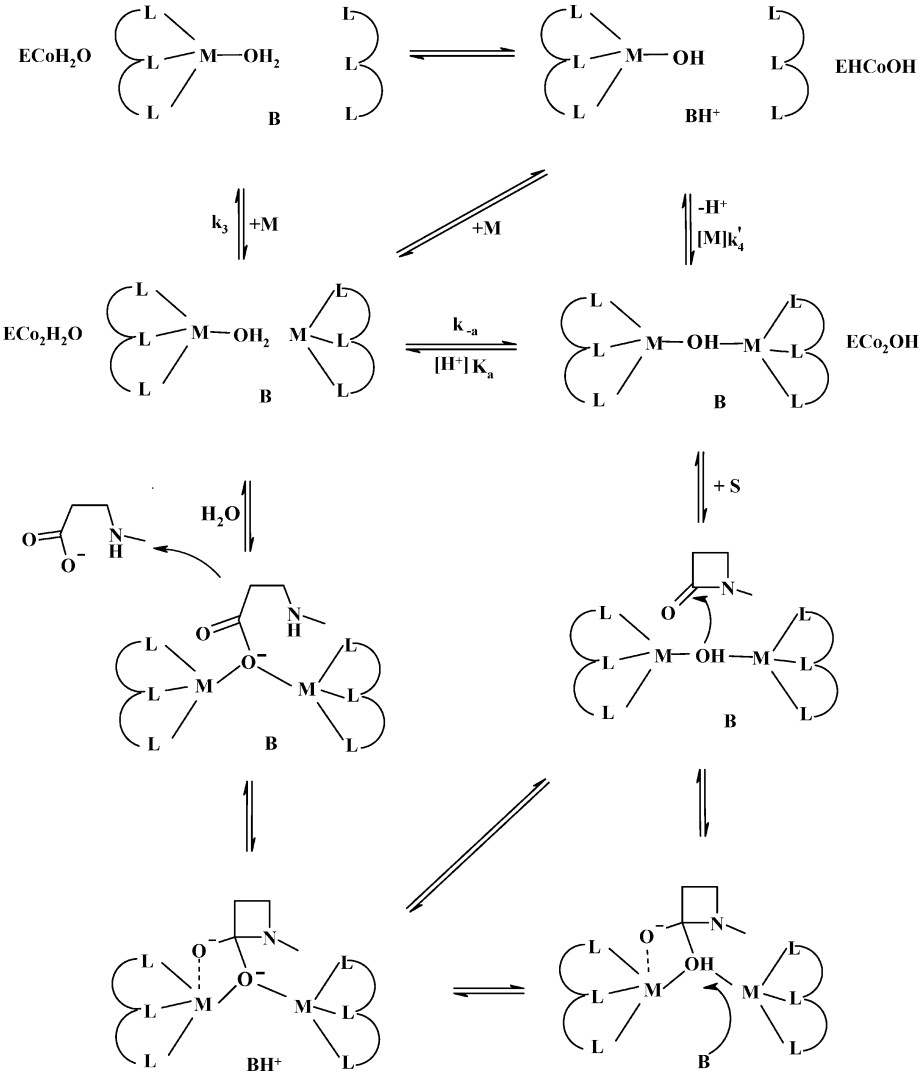

and ECoS. At lower pH, where k_3 is much greater than k_4, the main species at steady-state is the mono-cobalt enzyme (ECoS), whereas at higher pH, where k_3 decreases and k_4 increases, the steady-state is given by a mixture of di-cobalt (ECo_2S) and mono-cobalt enzymes (ECoS).

The magnitude of the burst, that is, the amount of product hydrolyzed during the pre-steady-state regime, is given by E_0k_2/k_3, when $k_4 \ll k_3$, so that as k_3 decreases at higher pH and k_2 is essentially constant, less enzyme is needed to get the same size of burst. Although pathway B in Scheme 5 is the simplest pathway from a mathematical point of view to treat the experimental data, the biphasic character of the progress curves can also be explained by other more complicated but kinetically indistinguishable schemes. For example, a different intermediate, ECo_2P or a free enzyme species, $EHCo_2$, could be responsible for the branch.

At the molecular level, Scheme 7 illustrates a possible mechanism for the CoBcII catalyzed hydrolysis of benzylpenicillin. The di-cobalt enzyme (ECo_2OH) binds the substrate and forms the Michaelis complex, followed by several chemical steps before the product is formed. Any one of the di-cobalt metalloenzyme species on the catalytic pathway is potentially able to lose one metal ion and give the catalytically less active (or inactive) mono-cobalt enzyme species and, consequently, the observed decrease in rate. For this to occur, the interaction of the second cobalt ion with the enzyme ligands and possibly the substrate must be reduced.

One chemically feasible possibility is that the branching occurs in the step involving regeneration of the catalytic metal-bridging hydroxide, which is consumed during turnover. For example, if product release occurs through displacement by water or if the water molecule bridging the two metal ions in ECo_2H_2O is introduced in a separate step following product release, deprotonation must occur to generate a catalytically active species (ECo_2OH) (Scheme 7). The deprotonation step (k_{-a}) may be in competition with metal-ion dissociation (k_3) so that after a number of k_{-a}/k_3 turnovers, the rate-limiting step becomes the association of the metal ion to the mono-cobalt enzyme to give the catalytically active di-cobalt enzyme (ECo_2OH). This mechanism explains the kinetic dependencies of the various derived rate constants.

There are many potential mechanistic roles for the metal ions in β-lactamases. It is commonly suggested that the metal ion lowers the pK_a of the coordinated water so that the metal-bound hydroxide ion is a better nucleophile than water itself. However, the lower the pK_a of metal-bound water, the more tightly bound and stabilized the resulting hydroxide ion, which, although it becomes the dominant species even at

low pH, corresponds to a more weakly nucleophilic hydroxide ion. If a major role of the metal ion is to provide a better nucleophile than water, then the net catalytic effect depends on the relative importance of concentration and the dependence of the rate upon nucleophilicity. If the pK_a is above the desired pH range, then metal-coordinated water will be the dominant species over the desired pH range, but deprotonation will give a more nucleophilic metal-bound hydroxide. How reactivity changes with changing pK_a and pH will depend on the susceptibility of the rate of reaction to the basicity of the nucleophile, the hydroxide ion bound to the metal, as indicated by the Bronsted β_{nuc} value. It is likely that a water molecule bound to two metal ions will have a lower pK_a than that bound to one. The other major role for the metal ion is to act as a Lewis acid by coordination to the β-lactam carbonyl oxygen giving a more electron deficient carbonyl carbon that facilitates nucleophilic attack. The metal ion, thus, stabilizes the negative charge developed on the carbonyl oxygen of the tetrahedral intermediate anion. Breakdown of the tetrahedral intermediate could also be facilitated by Lewis acid catalysis involving direct coordination of the departing amine nitrogen to the metal ion. A low pK_a implies a more electron deficient metal-ion center, which would give a better Lewis acid to stabilize the negative charge developed on the oxyanion of the tetrahedral intermediate. The di-cobalt β-lactamase from BcII, thus, presumably requires the metal ions to adopt both of these important catalytic roles.

In summary, we have shown that the biphasic kinetic behavior observed in the hydrolysis of benzylpenicillin catalyzed by cobalt substituted β-lactamase from *Bacillus cereus* is due to the loss of a metal ion from the active site of the di-cobalt enzyme to generate a catalytically inactive species. This is due to an intrinsic part of the mechanism, which requires the bridging hydroxide ion to be consumed during turnover. Hence, this catalytically important group has to be replaced by water, and its absence as a ligand for binding the metal ion gives the opportunity for competitive metal-ion dissociation from the enzyme. Preliminary studies suggest that these pathways also operate for the native zinc enzyme under certain conditions.

REFERENCES

1. Frère, J. M. (1995) Beta-lactamases and bacterial resistance to antibiotics, *Mol. Microbiol. 16*, 385−395.
2. Galleni, M., Lamotte-Brasseur, J., Rossolini, G. M., Spencer, J., Dideberg, O., and Frère, J. M. (2001) Standard numbering scheme for class B β-lactamases, *Antimicrob. Agents Chemother. 45*, 660−663.
3. Fabiane, S. M., Sohi, M. K., Wan, T., Payne, D. J., Bateson, J. H., Mitchell, T., and Sutton, B. J. (1998) Crystal structure of the zinc-dependent β-lactamase from *Bacillus cereus* at 1.9 Å resolution: binuclear active site with features of a mononuclear enzyme, *Biochemistry 37*, 12404−12411
4. Orellano, E. G., Girardini, J. E., Cricco, J. A., Ceccarelli, E. A., and Vila, A. J. (1998) Spectroscopic characterization of a binuclear metal site in *Bacillus cereus* β-lactamase II, *Biochemistry 37*, 10173−10180.
5. Paul-Soto, R., Bauer, R., Frère, J. M., Galleni, M., Meyer-Klaucke, W., Nolting, H., Rossolini, G. M., de Seny, D., Hernandez-Valladares, M., Zeppezauer, M., and Adolph, H. W. (1999) Mono- and binuclear Zn^{2+}-β-lactamase. Role of the conserved cysteine in the catalytic mechanism, *J. Biol. Chem. 274*, 13242−13249.
6. Concha, N. O., Rasmussen, B. A., Bush, K., and Herzberg, O. (1996) Crystal structure of the wide-spectrum binuclear zinc β-lactamase from Bacteroides fragilis, *Structure 4*, 823−836.
7. Paul-Soto, R., Hernadez-Valladares, M., Galleni, M., Bauer, R., Zeppezauer, M., Frère, J. M., and Adolph, H. W. (1998) Mono- and binuclear Zn^{2+}-β-lactamase from *Bacteroides fragilis*: catalytic and structural roles of the zinc ions, *FEBS Lett. 438*, 137−140.
8. Yang, Y., Keeney, D., Tang, X., Canfield, N., and Rasmussen, B. A. (1999) Kinetic properties and metal content of the metallo-β-lactamase CcrA harboring selective amino acid substitutions, *J. Biol. Chem. 274*, 15706−15711.
9. Wang, Z., Fast, W., and Benkovic, S. J. (1999) On the mechanism of the *Bacteroides fragilis* metallo-β-lactamase, *Biochemistry 38*, 10013−10023.
10. Laraki, N., Franceschini, N., Rossolini, G. M., Santucci, P., Meunier, C., de Pauw, E., Amicosante, G., Frère, J. M., and Galleni, M. (1999) Biochemical characterisation of the *Pseudomonas aeruginosa* 101/1477 metallo-β-lactamase IMP-1 produced by *Escherichia coli*, *Antimicrob. Agents Chemother. 43*, 902−906.
11. Haruta, S., Yamaguchi, H., Yamamoto, E. T., Eriguchi, Y., Nukaga, M., O'Hara, K., and Sawai, T. (2000) Functional analysis of the active site of a metallo-β-lactamase proliferating in Japan, *Antimicrob. Agents Chemother. 44*, 2304−2309.
12. Concha, N. O., Janson, C. A., Rowling, P., Pearson, S., Cheever, C. A., Clarke, B. P., Lewis, C., Galleni, M., Frère, J. M., Payne, D. J., Bateson, J. H., and Abdel-Meguid, S. S. (2000) Crystal structure of the IMP-1 metallo β-lactamase from *Pseudomonas aeruginosa* and its complex with a mercaptocarboxylate inhibitor: binding determinants of a potent, broad-spectrum inhibitor, *Biochemistry 39*, 4288−4298.
13. Garcia-Saez, I., Hopkins, J., Papamicael, C., Franceschini, N., Amicosante, G., Rossolini, G. M., Galleni, M., Frère, J. M., and Dideberg, O. (2003) The 1.5-A Structure of *Chryseobacterium meningosepticum* zinc β-Lactamase in complex with the inhibitor, D-captopril, *J. Biol. Chem. 278*, 23868−23873.
14. Crowder, M. W., and Walsh, T. R. (1999) Structure and function of metallo-β-lactamases, *Recent Res. Dev. Antimicrob. Agents Chemother. 3*, 105−132.
15. Carfi, A., Duee, E., Galleni, M., Frère, J. M., and Dideberg, O. (1998) 1.85 Å resolution structure of the zinc (II) β-lactamase from *Bacillus cereus*, *Acta Crystallogr., Sect. D 54*, 313−323.
16. Carfi, A., Duee, E., Paul-Soto, R., Galleni, M., Frère, J. M., and Dideberg, O. (1998) X-ray structure of the Zn(II) β-lactamase from *Bacteroides fragilis* in an orthorhombic crystal form, *Acta Crystallogr., Sect. D 54*, 45−57.
17. Concha, N. O., Rasmussen, B. A., Bush, K., and Herzberg, O. (1997) Crystal structure of the cadmium- and mercury-substituted metallo-β-lactamase from *Bacteroides fragilis*, *Protein Sci. 6*, 2671−2676.
18. Paul-Soto, R., Zeppezauer, M., Adolph, H. W., Galleni, M., Frère, J. M., Carfi, A., Dideberg, O., Wouter, J., Hemmingsen, L., and Bauer, R. (1999) Preference of Cd(II) and Zn(II) for the two metal sites in *Bacillus cereus* β-lactamase II: a perturbed angular correlation of γ-rays (PAC) spectroscopy study, *Biochemistry 38*, 16500−16506.
19. de Seny, D, Heinz, U., Wommer, S., Kiefer, M., Meyer-Klaucke, W., Galleni, M., Frère, J. M., Bauer, R., and Adolph, H. W. (2001) Metal ion binding and coordination geometry for wild type and mutants of metallo-β-lactamase from *Bacillus cereus 569/H/9* (BcII); a combined thermodynamic, kinetic and spectroscopic approach, *J. Biol. Chem. 276*, 45065−45078.
20. Wommer, S., Rival, S., Heinz, U., Galleni, M., Frère, J. M., Franceschini, N., Amicosante, G., Rasmussen, B., Bauer, R., and Adolph, H. W. (2002) Substrate activated zinc binding of metallo-β-lactamases; physiological importance of the mononuclear enzymes, *J. Biol. Chem. 277*, 24142−24147.
21. Crowder, M. W., Wang, Z., Franklin, S. L., Zovinka, E. P., and Benkovic, S. J. (1996) Characterization of the metal-binding sites of the β-lactamase from *Bacteroides fragilis*, *Biochemistry 35*, 12126−12132.
22. Fast, W., Wang, Z., and Benkovic, S. J. (2001) Familial mutations and zinc stoichiometry determine the rate-limiting step of nitrocefin hydrolysis by metallo-β-lactamase from *Bacteroides fragilis*, *Biochemistry 40*, 1640−1650.
23. Mitic, N., Smith, S. J., Neves, A., Guddat, L. W., Gahan, L. R., and Schenk, G. (2006) The catalytic mechanisms of binuclear metallohydrolases, *Chem. Rev.*, in press. Weston, J. (2005) Mode of action of bi- and trinuclear zinc hydrolases and their synthetic analogues, *Chem. Rev. 105*, 2151−2174.

24. Auld, D. S. (1995) Removal and replacement of metal ions in metallopepatidases, *Methods Enzymol. 248*, 228−242. Maret, W., and Vallee, B. L. (1993) Cobalt as probe and label of proteins, *Methods Enzymol. 226*, 52−71. Vila, A. J., and Fernandez, C. O. (1997) Alkaline transition of *Rhus vernicifera* stellacyanin, an unusual blue copper protein, *Biochemistry 36*, 10566−10570. Guo, J. Q., Wang, S. K., Dong, J., Qiu, H. W., Scott, R. A., and Giedroc, D. P. (1995) X-ray and visible absorption spectroscopy of wild-type and mutant T4 gene 32 proteins: His^{61}, not His^{81} is the nonthiolate zinc ligand, *J. Am. Chem. Soc. 117*, 9437−9440.
25. Bertini, I., Johnsson, B. H., Luchinat, C., Pierattelli, R., and Vila, A. J. (1994) Strategies of signal assignments in paramagnetic metalloproteins. An NMR investigation of the thiocyanate adduct of the cobalt (II) substituted human carbonic anhydrase II, *J. Magn. Reson., Ser. B 104*, 230−239. Oz, G., Pountney, D. L., and Armitage, I. M. (1998) NMR spectroscopic studies of I=1/2 metal ions in biological systems, *Biochem. Cell Biol. 76*, 223−234. Bennet, B., and Holz, R. C. (1997) EPR studies on the mono- and dicobalt(II)-substituted forms of the aminopeptidase from *Aeromonas proteolytica*. Insight into the catalytic mechanism of dinuclear hydrolases, *J. Am. Chem. Soc. 119*, 1923−1933.
26. Bauer, R., Adolph, H. W., Andersson, I., Danielsen, E., Formicka, G., and Zeppezauer, M. (1991) Coordination geometry for cadmium in the catalytic zinc site of horse liver alcohol dehydrogenase: studies by PAC spectroscopy, *Eur. Biophys. J. 20*, 215−221.
27. Bicknell, R., Knott-Hunziker, Y., and Waley, S. G. (1983) The pH-dependence of class B and class C β-lactamases, *Biochem. J. 213*, 61−66.
28. Baldwin, G. S., Edwards, G. F. StL., Kiener, P. A., Tully, M. J., Waley, S. G., and Abraham, E. P. (1980) Production of a variant of beta-lactamase II with selectively decreased cephalosporinase activity by a mutant of *Bacillus cereus* 569/H/9, *Biochem. J. 191*, 111−116.
29. Hemmingsen, L., Damblon, C., Antony, J., Jensen, M., Adolph, H. W., Wommer, S., Roberts, G. C. K., and Bauer, R. (2001) Dynamics of mononuclear cadmium beta-lactamase revealed by the combination of NMR and PAC spectroscopy, *J. Am. Chem. Soc. 123*, 10329−10335.
30. Damblon, C., Jensen, M., Ababou, A., Barsukov, I., Papamicael, C., Schofield, C. J., Olsen, L., Bauer, R., and Roberts, G. C. (2003) The inhibitor thiomandelic acid binds to both metal ions in metallo-beta-lactamase and induces positive cooperativity in metal binding, *J. Biol. Chem. 31*, 29240−29251.
31. Wang, Z., and Benkovic, S. J. (1998) Purification, characterization, and kinetic studies of a soluble *Bacteroides fragilis* metallo-β-lactamase that provides multiple antibiotic resistance, *J. Biol. Chem. 273*, 22402−22408.
32. Myers, J. L., and Shaw, R. W. (1989) Production, purification and spectral properties of metal-dependent β-lactamase from *Bacillus cereus*, *Biochim. Biophys. Acta 995*, 264−272.
33. Bicknell, R., and Waley, S. G. (1985) Cryoenzymology of *Bacillus cereus* β-lactamase II, *Biochemistry 24*, 6876−6887.
34. Bicknell, R., Schaffer, A, Waley, S. G., and Auld, D. S. (1986) Changes in the coordination geometry of the active-site metal during catalysis of benzylpenicillin hydrolysis by *Bacillus cereus* β-lactamase II, *Biochemistry 25*, 7208−7215.
35. Bounaga, S., Laws, A. P., Galleni, M., and Page, M. I. (1998) The mechanism of catalysis and the inhibition of the *Bacillus cereus* zinc-dependent β-lactamase, *Biochem J. 331*, 703−711.
36. Rasia, R. M., and Vila, A. J. (2004) Structural determinants of substrate binding to *Bacillus cereus* metallo-β-lactamase, *J. Biol. Chem. 279*, 26046−26051.
37. Schowen, K. B., and Schowen, R. L. (1982) Solvent isotope effects on enzyme systems, *Methods Enzymol. 87*, 551−606.
38. Badarau, A. (2006) Reactivity and Inhibition of Metallo-β-lactamases, Ph.D. Thesis, University of Huddersfield, Huddersfield, U.K.

BI0610146